ARMA 22–2204

Improved Upscaling Methods for Carbonate Rock Image Data

Anup Kumar Shahi and Anil Kumar
IITB-Monash Research Academy, Powai, Mumbai, India
Dept. of Earth Sciences, IIT Bombay Powai, Mumbai, India
Dept. of Civil Engineering, Monash University, Melbourne, Victoria, Australia
Kumar Hemant Singh
Dept. of Earth Sciences, IIT Bombay Powai, Mumbai, India
Ranjith Pathegama Gamage
Dept. of Civil Engineering, Monash University, Melbourne, Victoria, Australia

Copyright 2022 ARMA, American Rock Mechanics Association

This paper was prepared for presentation at the 56th US Rock Mechanics/Geomechanics Symposium held in Santa Fe, New Mexico, USA, 26-29 June 2022. This paper was selected for presentation at the symposium by an ARMA Technical Program Committee based on a technical and critical review of the paper by a minimum of two technical reviewers. The material, as presented, does not necessarily reflect any position of ARMA, its officers, or members. Electronic reproduction, distribution, or storage of any part of this paper for commercial purposes without the written consent of ARMA is prohibited. Permission to reproduce in print is restricted to an abstract of not more than 200 words; illustrations may not be copied. The abstract must contain conspicuous acknowledgement of where and by whom the paper was presented.

ABSTRACT

Volumetric image data of rocks often need sophisticated image processing steps in any rock physics and petrophysics workflow. While the segmentation is highly dependent on the quality of data, a trade-off between resolution and field of view is inevitable. This work attempts to resolve this using multiple-point statistics that have long been used for generating synthetic images, though mostly applied to sandstone rocks where the heterogeneity is significantly less than that of carbonates. These algorithms work by sequentially populating a grid to emulate the observed image. However, finding the optimum kernel parameters is crucial to capturing the spatial characteristics of the data. Also, when dealing with multiple images, finding a single set of kernel parameters might not be a trivial task. Further these methods work by computing a covariance kernel that scales as the third power with the number of training examples, thus not scaling well with the more data. Therefore, we seek to design a single image-based upscaling method that would help alleviate these difficulties. We test the proposed methodology on carbonate rock sample data which are known for their complexities at various scales. In this study images of 4 samples are considered. An upsample-deblur is developed that consistently works better than the conventional bicubic interpolation based upsampling technique. For this, a low-resolution 2D image sample is extracted from an X-ray microtomography dataset which was then subjected to a Random Forest based upsampling algorithm. It is found that the data from low scale could be improved to form a single super-resolution image. The algorithm produces an image that is always better than the bicubic algorithm. We anticipate this strategy would help design advanced algorithms where the amount of training examples is less.

Downloaded from http://onepetro.org/ARMAUSRMS/proceedings-pdf/ARMA22/All-ARMA22/ARMA-2022-2204/3064931/arma-2022-2204.pdf by China University of Petroleum (East China) user on 08 July 2023

1. INTRODUCTION

Digital Rock Physics workflow has gained significant attention from researchers due to its promising accuracy to characterize rocks and predict desired properties through numerical simulation (Andrä et al., 2013a, 2013b). Digital rock physics is a numerical workflow to compute and simulate various rock properties such as permeability, electrical conductivity, and elastic moduli based on high-resolution representations of the complex pore geometry obtained from imaging (Andrä et al., 2013a, 2013b; Arns et al., 2019; Devarapalli et al., 2017; Mehmani et al., 2020; Wildenschild & Sheppard, 2013).

X-Ray microcomputed tomography (Micro-CT) and Scanning Electron Microscopy (SEM) are widely used techniques to acquire digital rock images that aid in non-destructive testing of rock samples (Blunt et al., 2013; Prodanović et al., 2015). Despite all the advances in 3-dimensional imaging technique there exists a trade-off between field of view and voxel size which adversely affects the Digital Rock Physics Workflow (Latief et al., 2017; Wang et al., 2019). To accurately predict fluid flow properties, electrical conductivity and elastic moduli, an image with larger field of view and higher resolution is desirable which is not possible with single scale scan volume. Larger field of view (FOV) is required to precisely represent large pores in the samples and achieve the representative elementary volume (REV) while higher resolution is needed to resolve the micropores which could be the determining factor for electrical conductivity and fluid flow (Al-Ansi et al., 2013; Janssens et al., 2020).

An ideal case would have both of the qualities. This particularly (Larger FOV and higher resolution) become desirable when one intends to simulate the physics-based properties of carbonate reservoirs which exhibit heterogeneous pore space that vary at all scales of imaging. Due to the heterogeneity in pore space, pore-scale simulation of carbonate reservoirs poses great computational challenges particularly because of a wide range of pore shape variations.

It is also understood core samples are difficult to get because hydrocarbon exploration is an expensive industry. Given the heterogeneity, collection of a few core samples is generally not sufficient in case of carbonates. At this point it becomes very important to use the image data as carefully as possible. Modern day Deep-Learning algorithms require a large amount of data. This discourages the use as the images obtained of real core samples is usually small.

To overcome these challenge various researchers have used different techniques to generate a single image which has larger field of view with sufficient resolution to capture the microstructure of rocks using Machine Learning (Janssens et al., 2020; Niu et al., 2020; Shan et al., 2022; Wang et al., 2020) and Multipoint Statistics (Okabe & Blunt, 2005, 2007).

Our research focusses on a single image-based upscaling, where a Machine Learning model is developed to create a super resolution image. In this method the algorithm is made to learn a mapping from the low-resolution image to a high-resolution image. For this, the immediate local neighborhood of the concerned pixel is taken into consideration. In the first step the nearest neighbors are used to attain the required high-resolution size, then the details are added by the regression algorithm that is trained to map every pixel in the low-resolution image to its corresponding pixel in the high-resolution image. We illustrate the approach in the upcoming sections. While there is a marginal improvement in the upscaled image, the method fits itself well in low sample scenarios. We also anticipate that the procedure can greatly enhance other Deep-Learning based approaches that benefit from low sample set collections.

We base our development and motivation to work with as few examples as possible. It is known that images tend to exhibit structural similarity in the form of edges, corners and textures.

Authors in Buades et al. (2005) have used this property for denoising using local means. This work was then extended by Peyré et al. (2008) for optimization of inverse problems. Statistics should that these features tended to reoccur in small patches Glasner et. al (2009). This similarity can be explained for carbonate rock images like this – at the boundary of the pores the pixel values would have similar values along the edge whereas their variation would be high in other directions. Similarly, within the pores the pixels would bear similar values than non-porous regions. This implies that the detail of the structure is embedded into the surrounding pixels which can be exploited for regression based super-resolution. In the next section we give the methodology, discuss the results and provide some future developments in this regard.

Downloaded from http://onepetro.org/ARMAUSRMS/proceedings-pdf/ARMA22/All-ARMA22/ARMA-2022-2204/3064931/arma-2022-2204.pdf by China University of Petroleum (East China) user on 08 July 2023

2. METHODOLOGY

In this work we formulate the upscaling procedure as regression problem. For this we consider the random forest machine learning algorithm. They are essentially an ensemble of weak learners realized using decision trees.

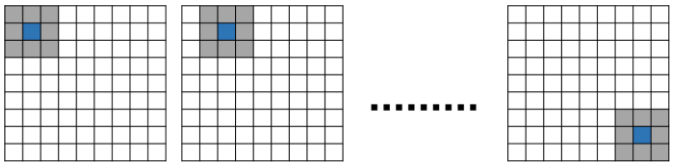

Fig. 1 Schematic representation of the steps for preparing the data for upscaling an image. The window of size 3×3 is slid with a step size 1 until all the pixels are covered. Blue center pixel is the target, and the surrounding grey pixels are predictors. Stacking all such pairs of target and predictors forms the supervised dataset for training.

The ensemble methods combine the predictive power of each of the weak learner to form one single strong learner. We make use of the random forests devised by Brieman (2001). The procedure randomizes both the training set as well as the splitting directions. This algorithm is particularly suitable for upscaling tasks because it lends itself well to large data. Moreover, the parameterization of the algorithm is small with just a few parameters (Liew et. al, 2002; Genuer et. al, 2002). Technically, we can define the regression using the following equations:

$$\mathrm{D_n} = \{(\mathrm{X_1}, \mathrm{y_n}), \dots, (\mathrm{X_n}, \mathrm{y_n})\} \qquad (1)$$

Where, D_n is a sample from the training set. The algorithm aims to output the response variable y given the regression function $m(x) = E[y|X = x]$. Here, E is the expectation operator. If the random forest is realized using M randomized decision trees, then the finite estimation of all of them can be given as:

$$\mathrm{m_{M,n}}(\mathrm{x}, \theta_1, \dots \theta_\mathrm{M}) = \frac{1}{\mathrm{M}} \sum_{\mathrm{j}=1}^{\mathrm{M}} \mathrm{m_n}(\mathrm{x}, \theta_\mathrm{j}) \qquad (2)$$

The prediction of the j^{th}tree in the forest for a point x is given as $m_n(x, \theta_j)$ where $\theta_1, \dots, \theta_M$ are independent random variables. Although there exist multiple ways of growing the trees, we follow the Brieman (2001) procedure where the splitting is done to minimize the variation among two resultant leaves. The algorithm is designed to stop when each leaf contains a pre-defined number of points.

In this work the random forest-based regression uses information from neighboring pixels to enhance the resolution of an image. For this the high-resolution image is predicted in patches from low resolution patches. By some experimentation we can find the suitable values of the parameters of the random forest. In Fig. 1 we show the steps for preparing the supervised dataset. A 3×3 size patch is extracted from the input image to form a predictor-target training pair. Therefore, in Eqn. 1 the y is the value of the target pixel shown in blue and X is the eight-dimensional predictor vector. The supervised set is formed by extracting the patches with a stride of size 1. The window of size 3 was found to be a nice trade-off between the enhancement quality and the training time. Higher values can help improve the technique further but at the cost of reduced number of training sets. The prediction of the high-resolution image is accomplished using a 2-stage process. Baker (2002) and Shan (2008) showed that the imaging process can be realized using a degradation of the continuous spatial domain depending on the point spread function of the camera. Technically, the process can be given as follows:

$$\mathrm{L_{img}} = (\mathrm{f_{blur}} * \mathrm{H}) \downarrow^{\mathrm{D}} \qquad (3)$$

Which can equivalently be written as

$$\widetilde{H}_{img} = f_{blur} * H \; and \; L_{img} = \widetilde{H} \downarrow^{D} \qquad (4)$$

Where $\downarrow^D$ denotes the downsampling function, L_{img}, H_{img} are low-resolution and high-resolution images, respectively. And f_{blur} denotes the blurring structuring element. The process of reversing the degradation process can be done in two steps – 1) upsampling of the L_{img} to obtain the $\widetilde{H}$; 2) use L_{img} and $\tilde{L}$ (the blurred version of L obtained by downsampling of $\widetilde{H}$) to refine the estimates over H. The 2-step process can be given by the flowchart shown in Fig. 2.

The process can be explained as follows: Starting from a low-resolution image, L_{img} we first upsample it using the basic bicubic interpolation scheme. Each pixel of this image is then predicted by a random forest regression model trained on a dataset of the low-resolution image (as shown in Fig. 1) to obtain $\widetilde{H}$. Then we blur the output image $\widetilde{H}$ using a Gaussian kernel and downsample it to obtain $\tilde{L}$.

Downloaded from http://onepetro.org/ARMAUSRMS/proceedings-pdf/ARMA22/All-ARMA22/ARMA-2022-2204/3064931/arma-2022-2204.pdf by China University of Petroleum (East China) user on 08 July 2023

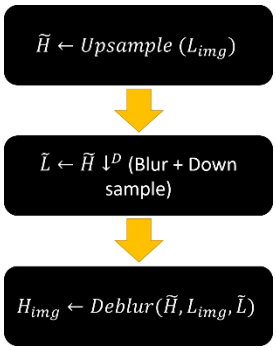

Fig. 2 Flowchart showing the upscaling scheme for single image super resolution. $\tilde{H}, H_{img}, \tilde{L}, L_{img}$ denote the blurred high-resolution image, high-resolution image, the blurred low-resolution image and low-resolution image, respectively.

In the third step, H_{img} is obtained by a deblurring operation which is realized using a second random forest regression algorithm that is trained on target-predictor pairs obtained from $\tilde{L}$.

The algorithm has been implemented using opensource Python libraries – Scikit Learn (Pedregosa et al., 2011), Matplotlib (Hunter et al., 2007) and simple slicing operations provided by the NumPy library (Harris et al. 2020). The random forest algorithm was implemented using the Scikit-Learn library; all the plotting was done using the Matplotlib library and the formation of the training set was done using the NumPy library.

3. METRICS FOR EVALUATING SUPER-RESOLVED IMAGE

Image quality assessment used to benchmark image processing algorithms. In the practice, image quality assessment for super-resolved images is twofold i.e., subjective evaluation based on human perception and objective evaluation based on quality metrics.

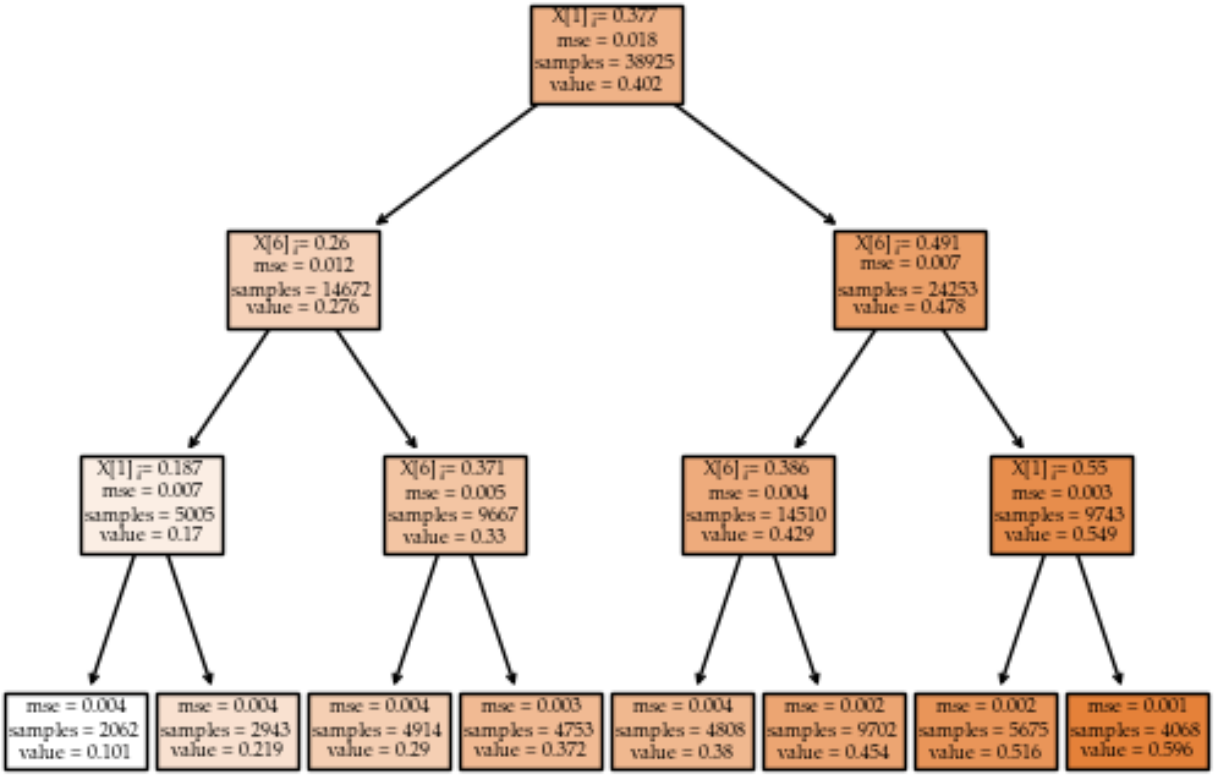

Fig.3 Sample of a decision tree from the trained random forest algorithm. Here, we show only three levels of decisions although the depth was set as 10 in the actual run.

For training the random forest algorithm the number of learners were kept as 100 and the maximum depth specified was 10. A sample of a trained decision tree can be seen in Fig. 3 where we curtail the last 7 levels of divisions for visualization purposes.

Among this method, the best reliable method for assessing the quality of images is subjective evaluation, it is a more direct way and is more in agreement with the practical requirement. However subjective evaluation has various limitations and user biasness, it is often time

Downloaded from http://onepetro.org/ARMAUSRMS/proceedings-pdf/ARMA22/All-ARMA22/ARMA-2022-2204/3064931/arma-2022-2204.pdf by China University of Petroleum (East China) user on 08 July 2023

consuming, expensive and cannot be automated hence cannot be integrated to real-time applications.
This type of assessment is also affected by lighting conditions and display devices.

Whereas objective evaluation is most convenient to employ, although the outcomes of various assessment metrics may not necessarily agree with each other as well as subjective assessment. Here, we use two commonly used metrics for assessment of objective quality (quantitative assessment indices) of super-resolved images; these two methods are Peak signal-to-noise ratio (PSNR) and structure similarity index (SSIM).

A) PSNR: Peak signal-to-noise ratio (PSNR) is the most widely used quantitative assessment indices for image restoration. For a given pixels within the images $\hat{X}$ and X, PSNR is defined as

$$\mathrm{PSNR} = 10.\log_{10}\left(\frac{\mathrm{L}^2}{\mathrm{MSE}}\right) \qquad (5)$$

where, MSE is mean squared error between pixels $\hat{X}$ and X and L is the maximum pixel value.

B) SSIM: The structure similarity index (SSIM) is another widely used quantitative assessment index that measures structural similarity. In SSIM, measurement or comparisons of image quality is based on the aspects of luminance, contrast, and structures.
The SSIM index is calculated on various windows of an image. The measure between two windows $\hat{X}$ and X of common size n-by-n is given by

$$\mathrm{SSIM}(\mathrm{X},\hat{\mathrm{X}}) = \frac{(2\mu_{\mathrm{X}}\mu_{\hat{\mathrm{X}}}+\mathrm{C}_1)(2\sigma_{\mathrm{X}\hat{\mathrm{X}}}+\mathrm{C}_2)}{(\mu_{\mathrm{X}}^2+\mu_{\hat{\mathrm{X}}}^2+\mathrm{C}_1))(\sigma_{\mathrm{X}}^2+\sigma_{\hat{\mathrm{X}}}^2+\mathrm{C}_2)} \qquad (6)$$

4. ROCK SAMPLE AND IMAGING

Image data used in this study is of Carbonate rock from the western offshore basin of India. The current research is based on core plugs acquired from highly heterogenous Limestone formation (Early Miocene Carbonates). The core plug used for micro-CT imaging in this study was cleaned using methanol and toluene to remove salt particles and organic particles from the pores. To ensure proper cleaning of the samples, a silver nitrate test was conducted after every 3-4 rounds of cleaning in the case of methanol; and discolouration of the solvent is observed in the case of toluene. After removing the samples from the Soxhlet, they were dried for 24 hours using a regular oven at 110^0 C and then placed in a furnace at 140^0 C for 6 hours.

The micro-CT scanner, GE 'v|tome|x', placed in the non-destructive lab at the central research facility of IIT Kharagpur, is used to acquire the image data of the rock core samples.

5. RESULTS

We have tested our machine learning based model on four sets of carbonate image data (viz. Sample ID 176, 259, 312 and 372) using Bicubic and Random Forest algorithm; their results for each data set are shown together for the comparison. The quality assessment metrics for the super-resolution image obtained from our algorithm is given in table 1.

Sample ID: 176

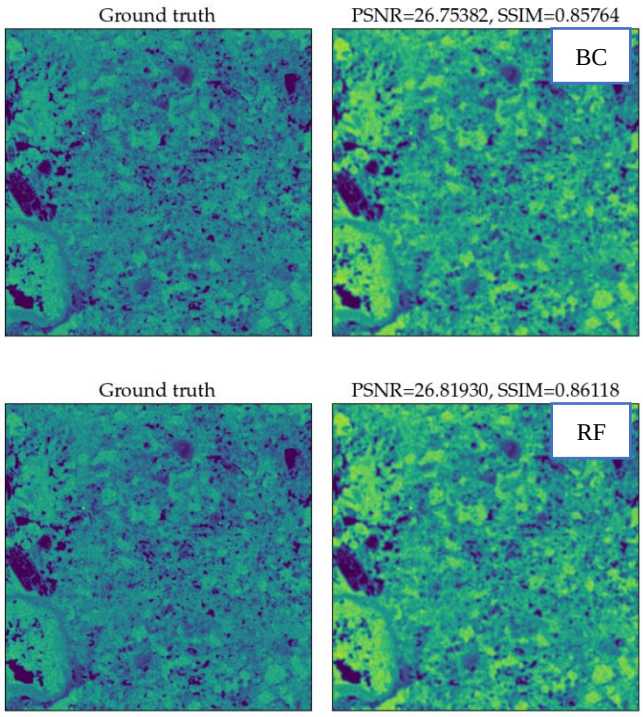

Fig. 4 Resulting super-resolution images obtained from bicubic interpolation, and Random Forest Regression. Annotation BC showing results for bicubic interpolation and RF for Random Forest algorithm.

Downloaded from http://onepetro.org/ARMAUSRMS/proceedings-pdf/ARMA22/All-ARMA22/ARMA-2022-2204/3064931/arma-2022-2204.pdf by China University of Petroleum (East China) user on 08 July 2023

Sample ID: 259

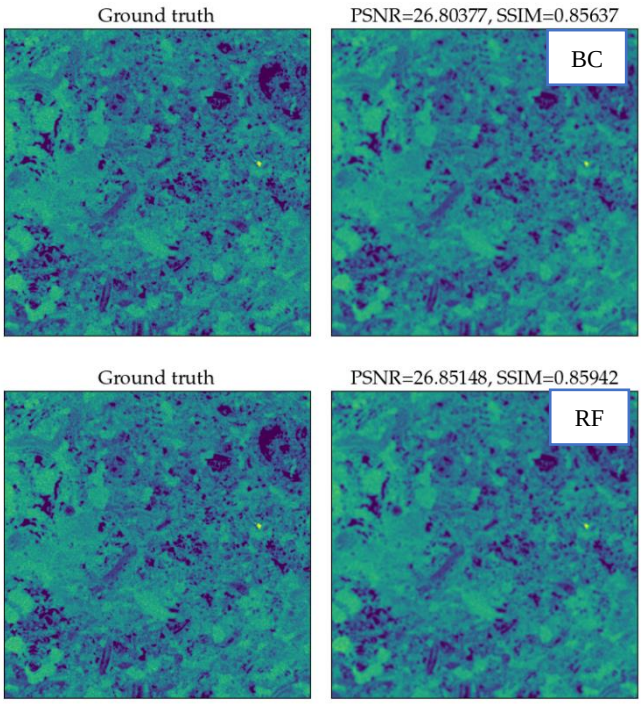

Fig. 5. Resulting SR images obtained from bicubic interpolation, and the Random Forest algorithm. Annotation BC showing results for bicubic interpolation and RF for Random Forest algorithm.

Sample ID: 312

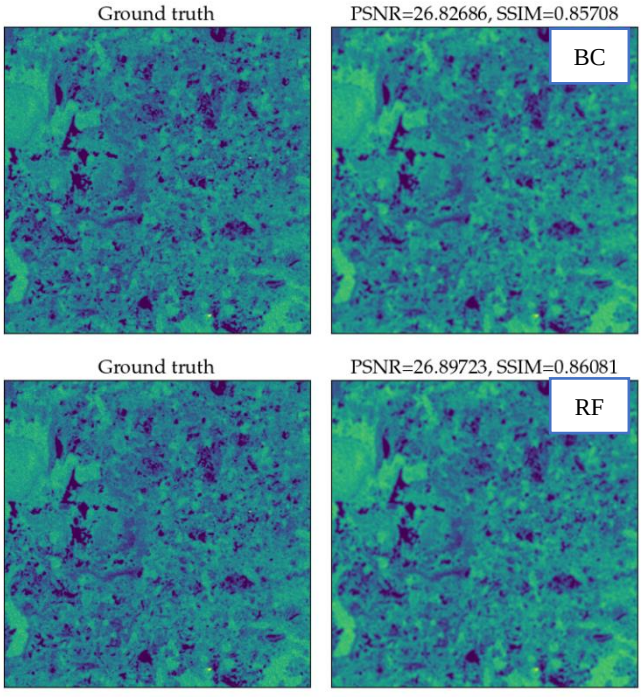

Fig. 6. Resulting SR images obtained from bicubic interpolation, and the Random Forest algorithm. Annotation BC showing results for bicubic interpolation and RF for Random Forest algorithm.

Sample ID: 372

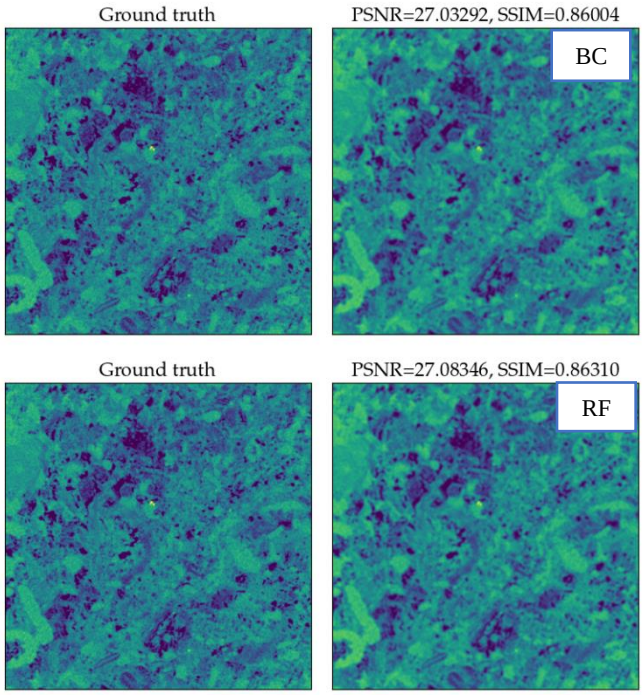

Fig. 7. Resulting SR images obtained from bicubic interpolation, and the Random Forest algorithm. Annotation BC showing results for bicubic interpolation and RF for Random Forest algorithm.

The generated SR image by the Random Forest algorithm interpolation model shows sharper details than the bicubic result as proven by the two metrics. The details about quantitative comparison between different models is shown in Table 1.

Table 1. Assessment metrics table for super resolved image by bi-cubic and random forest algorithm interpolation

Sample ID	Bi-cubic		Random Forest	
	PSNR	SSIM	PSNR	SSIM
176	26.753	0.857	26.819	0.861
259	26.803	0.856	26.851	0.859
312	26.826	0.857	26.897	0.86
372	27.032	0.86	27.083	0.863

6. CONCLUSIONS

This paper has worked out a way for doing single image super-resolution. Carbonate rocks sample images are known to exhibit extreme geometrical heterogeneity with no clear identifiable patterns. The degree of randomness increases with the increase in the field of view. While

Downloaded from http://onepetro.org/ARMAUSRMS/proceedings-pdf/ARMA22/All-ARMA22/ARMA-2022-2204/3064931/arma-2022-2204.pdf by China University of Petroleum (East China) user on 08 July 2023

there exist sophisticated Deep-Learning based algorithms (Wang et al., 2020) that can enhance/hallucinate the missing details in a low-resolution image, they still need quite an amount of data to build their knowledge repository. There also exist other methods which build image pyramids and/or use edge priors (Shan et al., 2022). Our method used the Random Forest algorithm-based regression to get a super-resolution image. Optimal tuning parameters (the number of estimators and the max tree depth) values are achieved by simple trials. The results shown here are from the best performing model. As discussed above the 8 surrounding pixels of the center pixel are helpful in enhancing the low-resolution image. We conclude that the spatial structure contains the necessary information to upscale a low-resolution image. For accomplishing the task, a machine learning algorithm such as the random forest algorithm can help leverage the crucial information from a few images and can be designed to accommodate more information from other training images to build a better super-resolution algorithm. We also anticipate that results of this work will help tweak the modern deep learning-based upscaling procedures to use as few training images as possible.

7. FUTURE WORK

Our work develops on the more realistic scenario where the data acquired is low in size. The current work just uses a single image to achieve a PSNR and SSIM that is better than the conventional Bi-cubic interpolation. We anticipate the inclusion of a "few" more examples would better enhance the details perceived in the super-resolution image. The current work can highly benefit the user (in low example data scenarios) when combined with deep learning upscaling algorithms such as the SRGAN and ESRGAN. We are currently working to develop the method.

8. REFERENCES

1. Al-Ansi, N., Gharbi, O., Raeini, A. Q., Yang, J., Iglauer, S., & Blunt, M. J. (2013). Influence of micro-computed tomography image resolution on the predictions of petrophysical properties. *Society of Petroleum Engineers - International Petroleum Technology Conference 2013, IPTC 2013: Challenging Technology and Economic Limits to Meet the Global Energy Demand*, *2*(Ic), 1291–1298.
2. Andrä, H., Combaret, N., Dvorkin, J., Glatt, E., Han, J., Kabel, M., Keehm, Y., Krzikalla, F., Lee, M., Madonna, C., Marsh, M., Mukerji, T., Saenger, E. H., Sain, R., Saxena, N., Ricker, S., Wiegmann, A., & Zhan, X. (2013a). Digital rock physics benchmarks-Part I: Imaging and segmentation. *Computers and Geosciences*, *50*, 25–32. https://doi.org/10.1016/J.CAGEO.2012.09.005
3. Andrä, H., Combaret, N., Dvorkin, J., Glatt, E., Han, J., Kabel, M., Keehm, Y., Krzikalla, F., Lee, M., Madonna, C., Marsh, M., Mukerji, T., Saenger, E. H., Sain, R., Saxena, N., Ricker, S., Wiegmann, A., & Zhan, X. (2013b). Digital rock physics benchmarks-part II: Computing effective properties. *Computers and Geosciences*, *50*, 33–43. https://doi.org/10.1016/j.cageo.2012.09.008
4. Arns, C. H., Jiang, H., Dai, H., Shikhov, I., SayedAkram, N., & Arns, J. Y. (2019). A digital rock physics approach to effective and total porosity for complex carbonates: Pore-Typing and applications to electrical conductivity. *E3S Web of Conferences*, *89*, 1–9. https://doi.org/10.1051/e3sconf/20198905002
5. Blunt, M. J., Bijeljic, B., Dong, H., Gharbi, O., Iglauer, S., Mostaghimi, P., Paluszny, A., & Pentland, C. (2013). Pore-scale imaging and modelling. *Advances in Water Resources*, *51*, 197–216. https://doi.org/10.1016/J.ADVWATRES.2012.03.003
6. Devarapalli, R. S., Islam, A., Faisal, T. F., Sassi, M., & Jouiad, M. (2017). Micro-CT and FIB–SEM imaging and pore structure characterization of dolomite rock at multiple scales. *Arabian Journal of Geosciences*, *10*(16). https://doi.org/10.1007/s12517-017-3120-z
7. Janssens, N., Huysmans, M., & Swennen, R. (2020). Computed tomography 3D super-resolution with generative adversarial neural networks: Implications on unsaturated and two-phase fluid flow. *Materials*, *13*(6). https://doi.org/10.3390/ma13061397
8. Latief, F. D. E., Fauzi, U., Irayani, Z., & Dougherty, G. (2017). The effect of X-ray micro computed tomography image resolution on flow properties of porous rocks. *Journal of Microscopy*, *266*(1), 69–88. https://doi.org/10.1111/jmi.12521
9. Mehmani, A., Verma, R., & Prodanović, M. (2020). Pore-scale modeling of carbonates. *Marine and Petroleum Geology*, *114*, 104141. https://doi.org/10.1016/j.marpetgeo.2019.104141
10. Niu, Y., Wang, Y. Da, Mostaghimi, P., Swietojanski, P., & Armstrong, R. T. (2020). An Innovative Application of Generative Adversarial Networks for Physically Accurate Rock Images With an Unprecedented Field of View. *Geophysical Research Letters*, *47*(23), e2020GL089029. https://doi.org/10.1029/2020GL089029
11. Okabe, H., & Blunt, M. J. (2005). Pore space

Downloaded from http://onepetro.org/ARMAUSRMS/proceedings-pdf/ARMA22/All-ARMA22/ARMA-2022-2204/3064931/arma-2022-2204.pdf by China University of Petroleum (East China) user on 08 July 2023

reconstruction using multiple-point statistics. *Journal of Petroleum Science and Engineering*, *46*(1–2), 121–137. https://doi.org/10.1016/j.petrol.2004.08.002

12. Okabe, H., & Blunt, M. J. (2007). Pore space reconstruction of vuggy carbonates using microtomography and multiple-point statistics. *Water Resources Research*, *43*(12). https://doi.org/10.1029/2006WR005680
13. Prodanović, M., Mehmani, A., & Sheppard, A. P. (2015). Imaged-based multiscale network modelling of microporosity in carbonates. *Geological Society Special Publication*, *406*(1), 95–113. https://doi.org/10.1144/SP406.9
14. Shan, L., Bai, X., Liu, C., Feng, Y., Liu, Y., & Qi, Y. (2022). Super-resolution reconstruction of digital rock CT images based on residual attention mechanism Digital rock super resolution reconstruction residual network attentional mechanism. *Advances in Geo-Energy Research*, *6*(2), 157–168. https://doi.org/10.46690/ager.2022.02.07
15. Wang, Y. Da, Armstrong, R. T., & Mostaghimi, P. (2019). Enhancing Resolution of Digital Rock Images with Super Resolution Convolutional Neural Networks. *Journal of Petroleum Science and Engineering*, *182*, 106261. https://doi.org/10.1016/j.petrol.2019.106261
16. Wang, Y. Da, Armstrong, R. T., & Mostaghimi, P. (2020). Boosting Resolution and Recovering Texture of 2D and 3D Micro-CT Images with Deep Learning. *Water Resources Research*, *56*(1). https://doi.org/10.1029/2019WR026052
17. Wildenschild, D., & Sheppard, A. P. (2013). X-ray imaging and analysis techniques for quantifying pore-scale structure and processes in subsurface porous medium systems. *Advances in Water Resources*, *51*, 217–246. https://doi.org/10.1016/j.advwatres.2012.07.018
18. Buades, A., Coll, B., & Morel, J. M. (2005, June). A non-local algorithm for image denoising. In 2005 IEEE Computer Society Conference on Computer Vision and Pattern Recognition (CVPR'05) (Vol. 2, pp. 60-65). IEEE.
19. Peyré, G., Bougleux, S., & Cohen, L. (2008, October). Non-local regularization of inverse problems. In European Conference on Computer Vision (pp. 57-68). Springer, Berlin, Heidelberg.
20. Glasner, D., Bagon, S., & Irani, M. (2009, September). Super-resolution from a single image. In 2009 IEEE 12th international conference on computer vision (pp. 349-356). IEEE.
21. Breiman, L. (2001). Random forests. Machine learning, 45(1), 5-32.
22. Liaw, A., & Wiener, M. (2002). Classification and regression by randomForest. R news, 2(3), 18-22.
23. Genuer, R., Poggi, J. M., & Tuleau, C. (2008). Random Forests: some methodological insights. arXiv preprint arXiv:0811.3619.
24. Baker, S., & Kanade, T. (2002). Limits on super-resolution and how to break them. IEEE Transactions on Pattern Analysis and Machine Intelligence, 24(9), 1167-1183.
25. Shan, Q., Li, Z., Jia, J., & Tang, C. K. (2008). Fast image/video upsampling. ACM Transactions on Graphics (TOG), 27(5), 1-7.
26. Harris, C. R., Millman, K. J., Van Der Walt, S. J., Gommers, R., Virtanen, P., Cournapeau, D., ... & Oliphant, T. E. (2020). Array programming with NumPy. *Nature*, *585*(7825), 357-362.
27. Pedregosa, F., Varoquaux, G., Gramfort, A., Michel, V., Thirion, B., Grisel, O., ... & Duchesnay, E. (2011). Scikit-learn: Machine learning in Python. *the Journal of machine Learning research*, *12*, 2825-2830.
28. Hunter, J. D. (2007). Matplotlib: A 2D graphics environment. *Computing in science & engineering*, *9*(03), 90-95.

Downloaded from http://onepetro.org/ARMAUSRMS/proceedings-pdf/ARMA22/All-ARMA22/ARMA-2022-2204/3064931/arma-2022-2204.pdf by China University of Petroleum (East China) user on 08 July 2023